Cracking and debonding of microlaminates

Z. Suo
Mechanical and Environmental Engineering Department, University of California, Santa Barbara, California 93106

(Received 8 October 1992; accepted 16 November 1992)

Materials layered together for their electronic properties and chemical stabilities are typically subjected to residual stresses induced by thermal expansion mismatch, epitaxy, phase transition, or other mechanisms specific to deposition procedures. Interacting with preexisting defects, these stresses can cause brittle layers to crack, or solid–solid interfaces to debond, which may be assisted by chemical reactions between atoms at the crack tip and species in the environment. Recent developments of fracture mechanics for layered materials are reviewed. Included are representative crack patterns, safety design criteria, crack driving force, and the physical origins of fracture resistance. The last section discusses unique mechanical properties of microlaminates.

I. INTRODUCTION

This article reviews recent results of Fracture Mechanics, addressing nonmechanics readers who, in the course of work related to layered materials, wish to grasp the essence of these results. Emphasis is placed on basic concepts; numerical and experimental works are cited directing to sources of further information.

The very smallness of electronic devices, as compared to structural components, leads to two unique characteristics. First, the elastic energy caused by mismatch strain is confined in small volumes of material, such as in a thin film. Second, fracture resistance is lower for a thin layered material than for bulk materials, because the former constrains plastic deformation. These two characteristics have the opposite trends: the first increases the residual stress sustainable by the system, and the second decreases it.

The general observation lends itself to a design criterion. To be definite, consider a film on a thick substrate, with mismatch strain ϵ_T, film thickness h, and Young's modulus of the film E_f. Let Γ be the energy needed to create a unit area of crack in the film, the substrate or the interface, depending on the crack location. The physical content of Γ is remarkably rich, which has been revealing itself over the last decade; we shall touch base with this line of investigation in a later section. At this point, however, Γ is simply regarded as a material property. In the absence of inelastic mechanisms to relax the mismatch strain, the elastic energy stored in the unit area of the film scales as $h\epsilon_T^2 E_f$; the thick substrate is essentially free of stress. Fracture releases the elastic energy by an amount $h\epsilon_T^2 E_f$ times the total crack area, with a dimensionless prefactor, Ω, which depends on the exact crack pattern. Fracture is avoided if Γ is larger than the elastic energy to be released, i.e.,

$$\frac{\Gamma}{h\epsilon_T^2 E_f} > \Omega. \tag{1}$$

This formula embodies the essentials of design against fracture in layered materials. To avoid cracking, one can reduce mismatch strain, reduce film thickness, increase fracture resistance, or use compliant materials.

A variety of crack patterns has been observed depending on tensile or compressive stress in the film. Figure 1 illustrates representative patterns caused by tensile stress in the film: channels in the film, spalling in the substrate, and debonding along the interface. The corresponding Ω is also listed, assuming similar elastic moduli for the film and substrate. Figure 2 illustrates a film under residual compression, buckling over a spot of radius R. An elementary consideration shows that the mismatch strain to cause buckling scales as

$$\epsilon_b \sim (h/R)^2, \tag{2}$$

with a prefactor close to unity, varying with the shape of the buckle. This failure mode happens only when both the buckling condition, $\epsilon_T > \epsilon_b$, and fracture condition, Eq. (1) are satisfied. The dimensionless number Ω in addition depends on the ratio ϵ_T/ϵ_b, and remains constant when $\epsilon_T/\epsilon_b > 2$.

The above outlines the framework to deal with fracture in microlaminates. For detailed evaluation of Ω, readers are referred to the review by Hutchinson and Suo,[1] and the contributions after that review on tensile films[2–4] and compressive films.[5,6] The following sections provide information on other quantities appearing in criterion, Eq. (1).

II. ENERGY BALANCE

Even a moment's thought shows that the fracture process must obey an energy balance:

work applied = (strain energy stored in the body)
+ (work of fracture).

But this does not take us very far. We want to determine how much load, or work, a device can sustain without fracture. Instead of answering the question, the above energy balance introduces two more quantities: strain energy and work of fracture (also known as fracture energy, fracture resistance, toughness).

Griffith[7] went one step further; his essential idea, after generations of scrutiny, goes as follows. Stress is intensified near the crack front, activating irreversible atomic movements within *thin* layers beneath the crack surfaces as the

 0734-2101/93/11(4)/1367/6/$1.00

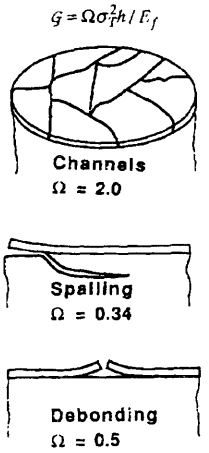

FIG. 1. Cracks caused by residual tension in the film.

front advances, leaving the rest of the device elastic. Taking advantage of these *boundary layers*, one defines work of fracture, Γ, as the work spent to create a unit area of the irreversible layers from the original material. For a device containing crack area A, loaded by force F, and work-conjugating displacement Δ, the energy balance becomes

$$Fd\Delta = dU + \Gamma dA, \tag{3}$$

where U is the elastic energy stored in the sample. In computing U, the thin irreversible layers are taken to be volumeless planes,and the entire device, down to the crack tip, is taken to be elastic. Obviously, this approach is meaningful only when each irreversible layer is much thinner than the film, which is often true because the former is of atomic dimension for brittle solids. (Progress has been made for situations where the boundary layer approach breaks down, which is out of the scope of this article and will not concern us here.) Consequently, U can be computed for any given load and geometry by standard elastic stress analysis, without referring to the irreversible process. The result, U, depends on Δ and A, varying as

$$dU = Fd\Delta - GdA. \tag{4}$$

That is, the strain energy equals the applied work when the crack size is held fixed, and has an extra contribution when the crack grows. All other quantities being specified, Eq. (4) defines G as the driving force for crack area A, having the dimension energy/area. Once U is computed, G is obtained by differentiation. Comparing Eqs. (3) and (4), one concludes that fracture will not proceed if

$$G < \Gamma. \tag{5}$$

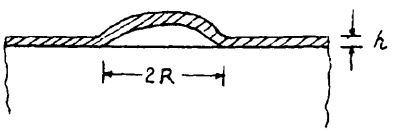

FIG. 2. Buckle-driven delamination for a film under residual compression.

Observe that the two quantities involve vastly different length scales: G the elastic energy change of the entire device, Γ the energy to rearrange atoms in the boundary layers, whose dimension is often of atomic dimension for brittle materials.

Now apply Griffith's general consideration to a thin film on a thick substrate. Dimensional considerations indicate that

$$G = \Omega h \epsilon_T^2 E_f, \tag{6}$$

where Ω is a dimensionless number, of order unity, depending on crack pattern and the ratio of elastic moduli of the film and substrate. Combining Eqs. (5) and (6) leads to criterion Eq. (1). The following two sections examine in some detail the physical origins of fracture driving force and resistance, G and Γ. The two sections are independent, to be read in any order.

III. FRACTURE DRIVING FORCE

A. Mismatch strain

Prevalent sources of mismatch include thermal expansion, epitaxy, sintering, and phase transition. The sign of the mismatch strain can be confusing; it is best judged by common sense.

Upon cooling, both the film and the substrate contract but by different amounts, giving rise to a mismatch strain

$$\epsilon_T = |\alpha_f - \alpha_s|(T_0 - T), \tag{7}$$

where α_f and α_s are the thermal expansion coefficients of the film and the substrate, T_0 is the temperature at which the film and substrate start to bond, and T is the current temperature.

For an epitaxial film–substrate, the difference in crystal lattice parameters induces a mismatch strain

$$\epsilon_T = |\alpha_s - \alpha_f|/\alpha_s, \tag{8}$$

where α_f and α_s are the lattice parameters of the film and substrate.

If the volume of the film tends to change after it has been bonded to the substrate, a mismatch strain results:

$$\epsilon_T = \theta/3, \tag{9}$$

where θ is volume shrinkage. This includes inorganic powder sintering and polymer crosslinking.

Phase transitions can also cause mismatch strain. Consider a thin ferroelectric film on a substrate, bonded at a temperature where the film is paraelectric. After cooling through the transition temperature under an electric field applied normal to the film, the film is polarized along the field direction. The change in lattice constant at the transition induces a strain

$$\epsilon_T = (\alpha_h - \alpha_l)/\alpha_l, \tag{10}$$

where α_h and α_l are the lattice parameters of high- and low-temperature phases, respectively.

B. Residual stress

Residual stresses in layered materials are reviewed in detail by Nix.[8] Even though powerful numerical-stress-analysis codes exist, computation of residual stress from mismatch strain proves to be very difficult, mainly because the mismatch strain can be partially relaxed by complicated nonlinear mechanisms such as dislocation motion and atomic diffusion, the details of which are hard to quantify for thin films. Nevertheless, stress state can be determined experimentally. A well-known procedure involves measuring the radius of curvature of the film–substrate wafer, R. Elementary plate theory gives the biaxial residual stress in the film

$$\sigma_T = \frac{H^2}{6Rh}\frac{E_s}{1-\nu_s}, \tag{11}$$

where E_s is Young's modulus, and ν_s Poisson's ratio of the substrate, and H is the thickness of the substrate ($H \gg h$). The formula connects the residual stress with the curvature at any moment, independent of nonlinear deformation history of the film.

Unrelaxed mismatch strain sets the upper bound to the residual stress level, and therefore leads to conservative design criteria. If the mismatch strain has been identified, the elastic stress can be computed, for any complex film architecture, by standard stress-analysis codes. For a continuous *thin* film on a *thick* substrate, the stress state at the edge of the film is complicated by the shape of the edge, which is uncertain in practice. Fortunately, most fracture criteria do not depend on these details. Attention is therefore focused on the stress state away from the edges. The thick substrate is essentially free of stress, so that the film is biaxially strained by ϵ_T from zero stress state. Hooke's law shows the biaxial stress in the film to be

$$\sigma_T = \epsilon_T E_f/(1-\nu_f), \tag{12}$$

where ν_f is Poisson's ratio of the film. For a stack of different films on a thick substrate, the residual stress in each film is still given by Eq. (12), where ϵ_T is the mismatch strain between this particular film and the substrate, as if all other films were absent.

C. Cracking number Ω: Films and vias

Once the mismatch strain is identified and the film is assumed to remain elastic, the dimensionless number Ω can be computed by standard numerical stress analysis codes. These analyses have been reviewed for representative cracking patterns,[1–6] and will not be repeated here. The concepts are applicable to other heterogeneous systems, e.g., a cylindrical conducting via embedded in an insulating substrate. Experimental studies of this configuration have been primarily conducted in the context of fiber reinforced composites, with fibers under either residual compression,[9] or residual tension.[10] Figure 3 reproduces the computed cracking number for the case where fiber is in compression, but the matrix sustains tensile stress in the hoop direction.[11] Evidently, both elastic mismatch and interface debonding affect matrix cracking. A crack pattern for vias under residual tension has also been analyzed.[12]

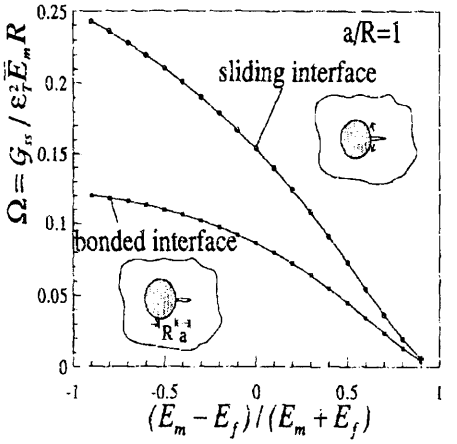

FIG. 3. A fiber under residual compression, embedded in an infinite matrix under residual tension in the hoop direction, causing a radial crack in the matrix.

IV. FRACTURE RESISTANCE

Experimental measurement of Γ is conceptually simple, but can be challenging because either samples are small, or data are complex to interpret. The subject has been reviewed by several groups.[13–15] Representative values are listed in Table I.

Attention of this section focused on theories that estimate Γ. Theories of fracture energy have been actively studied ever since Griffith made the proposition that Γ equals twice surface energy. The subject dominates the recent development of Fracture Mechanics for several reasons. First, various complex material systems, such as composites of various forms, offer opportunities of being tailored.[16] Second, other forms of energy supply in addition to tensile loading, such as shear loading,[17] electric fields,[18] and bond-weakening chemical reactions,[19] make fracture energy depend on too many variables to remain merely a phenomelogical quantity. Third, many toughened materials result in large inelastic zones, rendering the boundary layer approach inapplicable.[20] First principle calculations of macroscopic properties have always been complicated, be it elastic modulus, permittivity, or thermal conductivity. One should not expect the state of the affair to be different

TABLE I. Representative values of fracture energy.

Material	Γ(J/m^2)
SiO_2	1–10
Al_2O_3	30–50
Epoxy	~200
Au/Al_2O_3 interface	~50
Cu/SiO_2 interface	~10

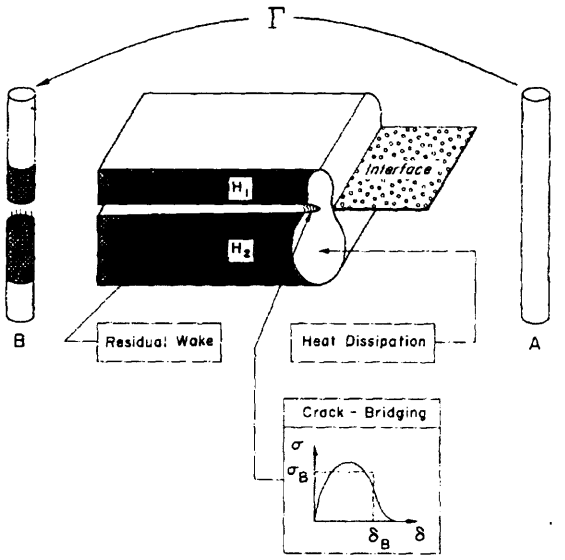

FIG. 4. Needleman's model.

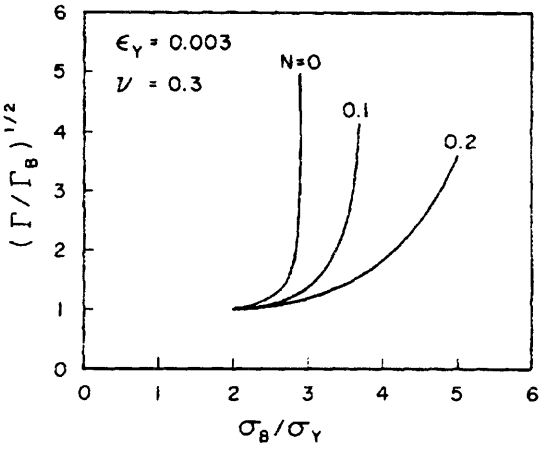

FIG. 5. Predictions on the basis of Needleman's model (Ref. 23).

for Γ. Nonetheless, a few idealized models will convey essentials. The following briefs one line of investigation.

Any model of fracture must explicitly identify two elements:

$$\text{fracture} = (\text{breaking bonds}) + (\text{creating irreversible layers}).$$

For brittle fracture involving only bond breaking over an atomic plane, the energy dissipation is simply the missing bonds on the crack planes. Higher fracture energy results if, somehow, atoms off the crack plane are persuaded to make irreversible movements. In fiber-reinforced ceramics, this is accomplished by frictional sliding between fibers and matrix. For a metal/ceramic bond, dislocation movements consume energy. Let Γ_B be the energy to break a bond, and Γ_P the plastic work; thus,

$$\Gamma = \Gamma_B + \Gamma_P. \tag{13}$$

Typically, plastic work dominates, i.e., $\Gamma_B \ll \Gamma_P$. All this has long been recognized. However, since inelastic deformation requires high stress to operate, the volume of atoms brought into dissipation is dictated by the bonding strength. That is, Γ_B, the smaller, dictates Γ_P, the bigger. Just how the two quantities are related remained unclear until recently.

A model is suggested by Needleman[21] on the basis of this conceptual picture. As illustrated in Fig. 4, the atomic cohesion is represented by an array of nonlinear springs, each characterized by a stress-separation law. The exact shape of the law is unimportant for the following discussion. Quantities that set the scale of cohesion are the bond strength, σ_B, and the interaction range, δ_B. The energy needed to separate the atomic plane, Γ_B, is the area under the force-separation curve, or approximately

$$\Gamma_B \sim \sigma_B \delta_B. \tag{14}$$

For inorganic materials, σ_B is about a tenth of Young's modulus, $\sigma_B \sim 10^{10}$ N/m^2; δ_B is around the atomic dimension, $\delta_B \sim 1$ Å. Thus, the decohesion energy is about $\Gamma_B \sim 1$ J/m^2, which agrees with the order of magnitude of the measured surface energies. Continuum plasticity is assumed to prevail in the background, responsible for energy dissipation. This model has since been interpreted for ceramic matrices containing both crack-bridging metal particles and phase-transforming ceramic particles,[22] and void growth in ductile alloys.[23] However, the model does not apply to the situation which it was originally intended for: atomic decohesion of metal/ceramic interfaces.

The yield strength of Cu, Al, Au, and Ag is on the order $\sigma_Y \sim 10^8$ N/m^2, much lower than atomic bond strength σ_B. According to Needleman's model, the crack tip blunts, limiting stress to about $3\sigma_Y$, so that decohesion is impossible within this framework. The inability of this model to account for atomic decohesion is further demonstrated by later calculations,[23] one of which is reproduced in Fig. 5. The hardening exponent for the metals cited above falls between $0 < N < 0.1$. The results in Fig. 5 may be summarized as

$$\Gamma/\Gamma_B \sim \begin{cases} 1, & \sigma_B/\sigma_Y < 2 \\ \infty, & \sigma_B/\sigma_Y > 3 \end{cases}.$$

The model suggests that in a fracture experiment, except for a narrow window, $2 < \sigma_B/\sigma_Y < 3$, one either measures cleavage energy or does not observe decohesion at all. In reality, atomic decohesion has been observed for a wide range of metal/ceramic interfaces, with a fracture energy substantially higher than the cleavage energy.[13,14]

The inability of this model to account for environmental cracking is also evident. In an ambient environment, the crack on a metal/ceramic interface grows under loads smaller than the failure load in an inert gas. The crack velocity increases rapidly with the magnitude of the load. Typically, a chemical reaction at the crack tip weakens the atomic bond. The transport of degrading species is assisted by partial opening of the atomic plane, the larger the load, the larger the opening, resulting in the observed velocity-

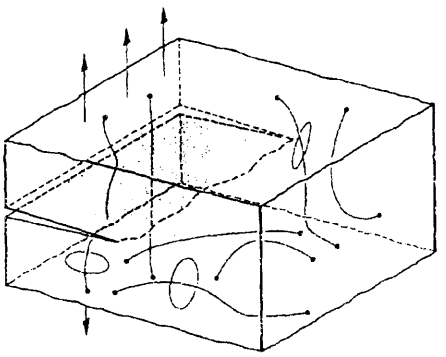

FIG. 6. A sharp crack front interacting with a dislocation network.

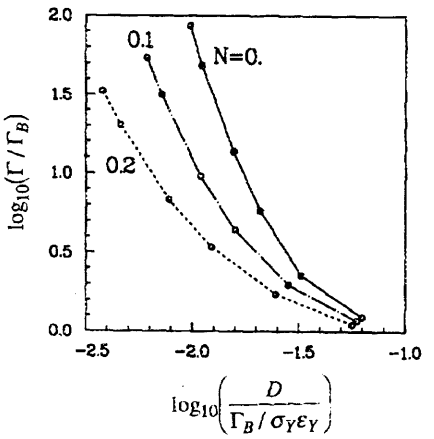

FIG. 7. Predictions of the elastic cell theory.

load relationship. However, Needleman's model would suggest that the crack tip blunts, limiting the near-tip stress to a few times yield stress independent of the applied load, so that the atomic plane opening will be very small and does not increase with the applied load.

The inadequacy of the model originates from its assumption; continuum plasticity cannot hold true down to the crack tip, at the atomic dimension. Figure 6 conveys the premise of a theory proposed by Suo, Shih, and Varias.[24] It is assumed that materials and testing conditions are such that no dislocation emits from the crack tip. This happens, for example, for interfaces subjected to environmental degradation, or interfaces with a few atomic monolayers of brittle reaction compounds to hinder dislocation emission. The problem becomes a sharp crack front interacting with a dislocation network. Two vastly different length scales are involved: the atomic dimension $b\sim10^{-10}$ m, and dislocation spacing $D\sim10^{-6}$ m. So long as $D\gg b$, the probability for a preexisting dislocation to blunt a major portion of the crack front should be extremely small. An elastic cell, of size D, therefore surrounds the crack tip, keeping the crack front sharp. A more remarkable role played by this micron-sized cell is that it mediates a huge stress gradient. This is understood as follows. Since the radii of both the crack front and individual dislocation are of atomic dimension, the classical elasticity solution is valid in the annulus between b and D, governed by the square-root decay:

$$\sqrt{D/b}\sim\sqrt{10^{-6}/10^{-10}}\sim100.$$

This decay is just what is needed: the high cohesive stress, prevailing at atomic dimension at the crack front, merges to the low yield strength outside the elastic cell.

A model convenient for calculation has been suggested on the basis of the elastic cell theory,[24] where an elastic cell of size D is assumed to surround the crack tip, and continuum plasticity prevails outside of the cell, with yield stress σ_Y and yield strain ϵ_Y. The crack tip fracture process is characterized by cohesive energy Γ_B. An important length scale emerges

$$H_B=\frac{1}{3\pi}\frac{\Gamma_B}{\sigma_Y\epsilon_Y}, \tag{15}$$

which is about the height of plastic zone at the onset of crack growth; for typical materials, $H_B\gg D$. As the crack grows, the height of the plastic layer increases, so is the applied load necessary to maintain the growth. A steady growth ensues after the crack extends by many H_B, wherein both the applied load and height of the plastic layer remain invariant. The steady-state load corresponds to the fracture energy of the material, Γ. Computed results can be summarized by the ratio Γ/Γ_B as a function of D/H_B (Fig. 7). The height of the steady-growing plastic layer is well estimated by Eq. (15), with Γ_B replaced by Γ.

V. CRACK AND DISLOCATION CONFINEMENT

The unique behaviors of layered materials present a *challenge* and also an *opportunity*. The former has been discussed in length, but the latter almost unexplored. Microlaminates exhibit high mechanical strength under stresses along the layers,[25] and high dielectric strength under electric fields normal to the layers.[18] The following briefly discusses superior mechanical properties of microlaminates.

A bulk ceramic may have high strength, but no ductility. A bulk metal may have large ductility, but the strength is limited. A material consisting of alternating submicron layers of metal and ceramic can attain an elastic limit much higher than both, but still have appreciable ductility. Microlaminates are therefore extremely creep/fatigue resistant. This effect can be understood as follows. For a thick metal, the elastic limit is the stress needed to bow out a dislocation between obstacles, such as precipitates:

$$S\sim\mu b/L. \tag{16}$$

Here μ is the shear modulus, b the atomic dimension, and L the obstacle spacing. If the thickness of the metal layer, h, is small, the adjacent ceramic layers serve as strong obstacles, confining the dislocation to tunnel within the metal layer. Now L should be replaced by h. When h is small, the elastic limit can be very large. The situation in a

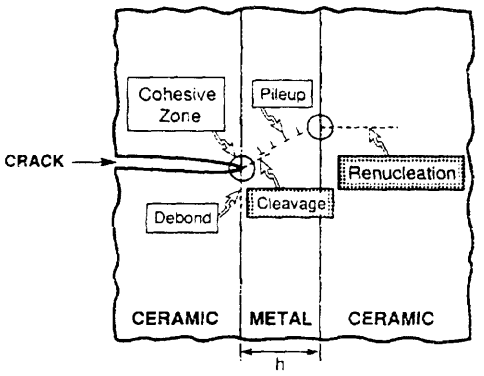

FIG. 8. Competing nonlinear mechanisms for submicron laminates.

ceramic layer is analogous. For a thick ceramic, the strength is governed by crack size, L, which scales with grain diameter,

$$S \sim \sqrt{\Gamma E/L}. \tag{17}$$

When layer thickness h is small, the crack is confined by the adjacent metal layers to tunnel in the ceramic layer, and L is now replaced by h. When h is small, the strength can be very high.

To have ductility, various nonlinear mechanisms are important. When a crack from a ceramic layer hits the interface, several things may happen: interface debond, dislocation pileup in metal, metal cleavage, and crack renucleation in the adjacent ceramic layer (Fig. 8). At submicron scales, the individuality of dislocations may become important, but the individuality of atoms may not. Significant dissipation is accomplished by dislocation motions at *multiple* crack sites. This requires that ceramic layers have large statistical distribution in strength, so that a crack in one ceramic layer does not cause a crack in nearby ceramic layers in proximity.

VI. CONCLUDING REMARKS

Fracture mechanics aims to relate fracture patterns at device level to micromechanisms of dissipation, and to cohesion and degredation processes at the atomic scale. Several length scales are involved, each sustaining a different stress level. A substantial body of knowledge has been synthesized by a framework of fairly uniform viewpoint. However, like any complex engineering problem, a good design of a device comes from semi-informed guesswork, and an amount of labor depending on how much detail one needs to resolve. An all-embracing, foolproof approach is not expected even in an age of elaborate computers and testing machines.

ACKNOWLEDGMENTS

The work reported here has been supported by NSF through a series of grants on mechanics problems in integrated circuits and high-performance composites. The author is most grateful for this support. Section IV is an abridged version of an article (Ref. 17) written in collaboration with Professor C. F. Shih.

[1]J. W. Hutchinson and Z. Suo, Adv. Appl. Mech. **29**, 63 (1992).
[2]J. L. Bueth, Int. J. Solids Struct. **29**, 1657 (1992).
[3]T. Ye, Z. Suo, and A. G. Evans, Int. J. Solids Struct. **29**, 2639 (1992).
[4]M. D. Thouless, E. Olsson, and A. Gupta, Acta Metall. Mater. **40**, 1287 (1992).
[5]J. W. Hutchinson, M. D. Thouless, and E. G. Liniger, Acta Metall. Mater. **40**, 259 (1992).
[6]M. D. Thouless, J. W. Hutchinson, and E. G. Liniger, Acta Metall. Mater. **40**, 2639 (1992).
[7]A. A. Griffith, Philos. Trans. R. Soc. London Ser. A **221**, 163 (1921).
[8]W. D. Nix, Metall. Trans. A **20**, 2217 (1989).
[9]T. C. Lu, J. Yang, Z. Suo, A. G. Evans, R. Hecht, and R. Mehrabian, Acta Metall. Mater. **39**, 1883 (1991).
[10]D. R. Clarke and Y. H. Chiao, Acta Metall. Mater. **38**, 259 (1990).
[11]S. Ho and Z. Suo, Acta Metall. Mater. **40**, 1685 (1992).
[12]L. B. Freund, and K. S. Kim, Mater. Res. Soc. Symp. Proc. **226**, 291 (1991).
[13]A. G. Evans, M. Ruhle, B. J. Dalgleish, and P. G. Charalambides, Mater. Sci. Eng. A **126**, 53 (1990); J. B. Davis, H. C. Cao, G. Bao, and A. G. Evans, Acta Metall. Mater. **39**, 1019 (1991); I. E. Reimanis and B. J. Dalgleish, *ibid.* **39**, 3133 (1991).
[14]R. M. Cannon, B. J. Dalgleish, R. H. Dauskardt, R. M. Fisher, T. S. Oh, and R. O. Ritchie, in *Fatigue of Advanced Materials*, edited by R. O. Ritchie, R. H. Dauskardt, and B. N. Cox (MCEP, Edgbaston, UK, 1991).
[15]K. S. Kim, Mater. Res. Soc. Symp. Proc. **203**, 3 (1991).
[16]A. G. Evans, J. Am. Ceram. Soc. **73**, 187 (1990).
[17]Z. Suo and C. F. Shih, in *Metal-Matrix Composites*, edited by S. Suresh, A. Mortensen, and A. Needleman (Butterworth-Heinemann, Stoneham, MA, 1992).
[18]Z. Suo, J. Mech. Phys. Solids (submitted).
[19]B. R. Lawn and T. R. Wilshaw, *Fracture of Brittle Solids* (Cambridge University Press, Cambridge, UK, 1975).
[20]G. Bao and Z. Suo, Appl. Mech. Rev. **45**, 355 (1992).
[21]A. Needleman, J. Appl. Mech. **54**, 525 (1987).
[22]J. C. Amazigo and B. Budiansky, J. Mech. Phys. Solids **36**, 1377 (1988).
[23]V. Tvergaard and J. W. Hutchinson, J. Mech. Phys. Solids **40**, 1377 (1992).
[24]Z. Suo, C. F. Shih, and A. G. Varias, Acta Metall. Mater. (in press).
[25]A. G. Evans (private communication).